



# Metal sources for the polymetallic Ni–Mo–PGE mineralization in the black shales of the Lower Cambrian Niutitang Formation, South China



Tao Han <sup>a,\*</sup>, Xiaoqing Zhu <sup>a</sup>, Kun Li <sup>b</sup>, Lei Jiang <sup>b</sup>, Chenghai Zhao <sup>a,c</sup>, Zhonggang Wang <sup>a</sup>

<sup>a</sup> State Key Laboratory of Ore Deposit Geochemistry, Institute of Geochemistry, Chinese Academy of Sciences, Guiyang 550002, China

<sup>b</sup> No. 104 Geological Team, Bureau of Geology and Mineral Exploration and Development of Guizhou Province, Duyun 558000, China

<sup>c</sup> University of Chinese Academy of Sciences, Beijing 100049, China

## ARTICLE INFO

### Article history:

Received 24 March 2014

Received in revised form 17 November 2014

Accepted 20 November 2014

Available online 6 December 2014

### Keywords:

Polymetallic Ni–Mo–PGE mineralization

Lower Cambrian

Black shales

TOC

Trace elements

## ABSTRACT

Total organic carbon content (TOC), trace element and platinum-group element (PGE) concentrations were determined in the black shales of the Lower Cambrian Niutitang Formation in the Nayong area, Guizhou Province, South China, in order to study the polymetallic Ni–Mo–PGE mineralization. The results demonstrate that numerous elements are enriched in the polymetallic ores compared to those of the nearby black shale, particularly Ni, Mo, Zn, TOC and total PGE, which can reach up to 7.03 wt.%, 8.49 wt.%, 11.7 wt.%, 11.5 wt.% and 943 ppb, respectively. The elemental enrichment distribution patterns are similar to those in the Zunyi and Zhangjiajie areas except that the Nayong location is exceptionally enriched in Zn. Whereas positive correlations are observed between the ore elements of the polymetallic ores, no such correlations are observed in the black shale. These positively correlated metallic elements are classified into three groups: Co–Ni–Cu–PGE, Zn–Cd–Pb and Mo–Tl–TOC. The geological and geochemical features of these elements suggest that Proterozoic and Early Palaeozoic mafic and ultramafic rocks, dolomites and/or Pb–Zn deposits of the Neoproterozoic Dengying Formation and seawater could be the principal sources for Co–Ni–Cu–PGE, Zn–Cd–Pb, and Mo–Tl–TOC, respectively. Furthermore, the chondrite-normalized patterns of PGEs with Pd/Pt, Pd/Ir and Pt/Ir indicate that PGE enrichment of the polymetallic ores is most likely related to hydrothermal processes associated with the mafic rocks. In contrast, PGE enrichment in the black shale resembles that of the marine oil shale with terrigenous and seawater contributions. Our investigations of TOC, trace elements and PGE geochemistry suggest that multiple sources along with submarine hydrothermal and biological contributions might be responsible for the formation of the polymetallic Ni–Mo–PGE mineralization in the black shales of the Lower Cambrian Niutitang Formation across southern China.

© 2014 Elsevier B.V. All rights reserved.

## 1. Introduction

Black shale is a dark, thinly laminated carbonaceous rock that is exceptionally rich in organic matter and sulfide, containing unusual concentrations of certain trace elements that tend to accumulate in a great variety of environments under suboxic through anoxic to euxinic conditions. In some cases, elemental enrichment in black shale may lead to the formation of giant ore deposits such as the Paleoproterozoic Ni–Cu–Zn–Co deposit of the Talvivaara mine in Finland (Loukola-Ruskeeniemi and Lahtinen, 2013), the Neoproterozoic Sukhoi Log gold deposit in Siberia (Distler et al., 2004) and the Late Permian Cu–Pb–Zn–PGE–Au deposit of the Kupferschiefer in Poland and Germany (Blundell et al., 2003). In southern China, an extraordinary layer hosted in Lower Cambrian black shales (a suite of rocks including black shale, Ni–Mo–PGE ores and other rocks) is rich in elements associated with felsic rocks (Mo–Pb–Zn–REE) and elements associated with mafic–

ultramafic rocks (Fe–Ni–Cu–PGE). This unique mineral system is known as polymetallic Ni–Mo–PGE ores (Zhang et al., 2002). In general, the widespread Lower Cambrian black shales and the accompanying economic mineralization are mainly distributed along the southern margin of the Yangtze Craton in the provinces of Yunnan, Guizhou, Hunan, Jiangxi and Zhejiang (Fig. 1).

During the past four decades, significant progress has been made in understanding the origin of the Ni–Mo–PGE mineralization because of efforts that were largely focused on the Zunyi area, Guizhou Province and the Zhangjiajie area, Hunan Province; however, uncertainties still remain. An early study suggested the possibility of an asteroid impact origin on the basis of the Ir anomaly, which can reach up to 31 ppb (Fan et al., 1987). Nonetheless, subsequent results showed an absence of Ir anomaly and did not support this hypothesis. Instead, published data indicated a submarine hydrothermal exhalative origin (Coveney and Chen, 1991; Coveney et al., 1992; Jiang et al., 2003; Li et al., 2003; Lott et al., 1999; Murowchick et al., 1994 and Steiner et al., 2001). In addition, several studies have proposed that the polymetallic ores were derived from seawater on the basis of trace elements, PGE and Mo

\* Corresponding author. Tel.: +86 851 5891199; fax: +86 851 5891664.  
E-mail address: [hantao@mail.gyig.ac.cn](mailto:hantao@mail.gyig.ac.cn) (T. Han).

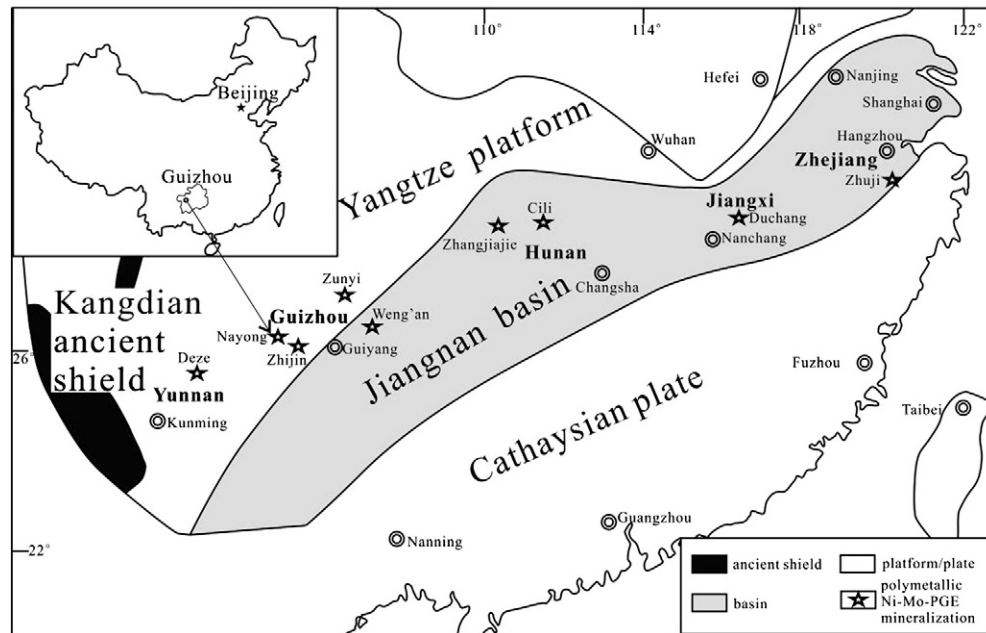


**Fig. 1.** Lithofacies palaeogeography map of the Early Cambrian and the distribution of polymetallic Ni–Mo–PGE mineralization, in South China (modified from Feng et al., 2002 and Mao et al., 2002).

isotope geochemistry (Lehmann et al., 2007; Mao et al., 2002 and Xu et al., 2012). Coveney (2003) and Jiang et al. (2006, 2007) suggested a submarine hydrothermal origin for the Ni–Mo–PGE ores on the basis of trace elements and PGE geochemistry. Moreover, mixing of seawater and terrigenous and hydrothermal sources has also been proposed (Pařava et al., 2008).

During the field investigation of the Ni–Mo–PGE mineralization of the Lower Cambrian black shales in southern China, some differences were observed in the poorly known mineralized site in Nayong, Guizhou Province compared to the well-studied Zunyi and Zhangjiajie areas. Thus, in the present paper, we examine the trace elements, PGE and TOC in the black shales of the Lower Cambrian Niutitang Formation in Nayong and discuss our findings for this type of mineralization. Moreover, the correlations between the enriched elements in the black shales of the Lower Cambrian Niutitang Formation in the Nayong area have also been used to elucidate metal sources for the polymetallic Ni–Mo–PGE mineralization along with its origin.

## 2. Geological setting

### 2.1. Regional geology

The black shales of the Lower Cambrian in southern China are located on the southern margin of the Yangtze Platform in the transition zone between the Yangtze Platform and the Jiangnan Basin (Gao and Li, 1998). In Early Cambrian, the Yangtze Platform was essentially dominated by fine-grained sandstone, siltstone and shale provided by the erosion of the nearby Kangdian Shield. The Jiangnan Basin contains shale, chert, stone coal and thin carbonate lenses (Fig. 1; Feng et al., 2002). The Ni–Mo–PGE mineralization in the Deze, Nayong, Zhijin, Zunyi, Weng'an, Zhangjiajie, Cili, Duchang and Zhuji areas is common in the black shales of the Lower Cambrian Niutitang Formation. Moreover, these mineralization sites form a linear belt from SW to NE.

The Lower Cambrian black shales in the Nayong area are located in the western part of the Guizhou province and the south-western part of the Yangtze Platform. Our studies were carried out on the Ni–Mo–PGE mineral systems in the mine area located in Shuidong town, which is about 20 km southeast from Nayong county. In the mining area, the exposed strata are primarily represented by the Upper

Neoproterozoic Dengying Formation, the Lower Cambrian Niutitang and the Mingxinsi Formations (Fig. 2). The Ni–Mo–PGE mineral systems are exclusively hosted in the Lower Cambrian Niutitang Formation. In addition, other small mineral occurrences are also present in the Nayong area, such as the Pb–Zn deposits, in the Neoproterozoic Dengying Formation (Fig. 2). The regional structures are dominated by the NE-trending faults (Shuidong fault, Pa'na fault and Dengjiazhai fault), the N–S faults (Qikeshu fault) and the NW-trending faults that control the distribution of these Pb–Zn deposits (Fig. 2). Minor occurrences of igneous rocks (Emeishan basalt and diabase) are also present in the northeast of the mining district (Fig. 2).

### 2.2. Geological characteristics of the polymetallic Ni–Mo–PGE mineral systems

From the bottom to the top, the black shales of the Lower Cambrian Niutitang Formation in the Nayong area can be divided into six lithological members (Fig. 3). (1) A ferruginous clay layer (0.1–0.5 m thick) in unconformable contact with the underlying dolomite of the Neoproterozoic Dengying Formation. (2) A thin discontinuous phosphate layer (0–0.5 m thick), e.g. in the drill cores that we examined, no phosphate layer was found (Fig. 3). (3) A laminated lower black shale ( $\geq 2$  m thick) with pyrite and apatite nodules. (4) A grey–black coarse-grained limestone (0.1–0.6 m thick) in which the size of the calcite grains is up to several millimetres and gradually decreases from bottom to top. (5) The Ni–Mo–PGE ore body (0.02–0.6 m thick) with several clasts and nodules of sulfides, apatite and organic matter. Finally, (6) a laminated upper black shale ( $\geq 5$  m thick) with pyrite nodules, thin pyrite and calcite veins that is in conformable contact with the upper Mingxinsi Formation (Fig. 3).

Two types of mineable bodies exist in the Nayong area. The first is mainly parallel to the flat-lying strata as in the Zunyi and Zhangjiajie areas (Fig. 4a), whereas the second is perpendicular to the strata (Fig. 4b). The textures of these two types of polymetallic ores in the Nayong area are very similar to those in the Zunyi and Zhangjiajie deposits that commonly have banded and lenticular structures (Fig. 4c and d). The ore minerals, such as MoSC, millerite, sphalerite, pyrite and apatite, are present as scattered clasts and nodules in the silicate matrix (Fig. 4e, f). Amorphous MoSC, with an approximate formula of

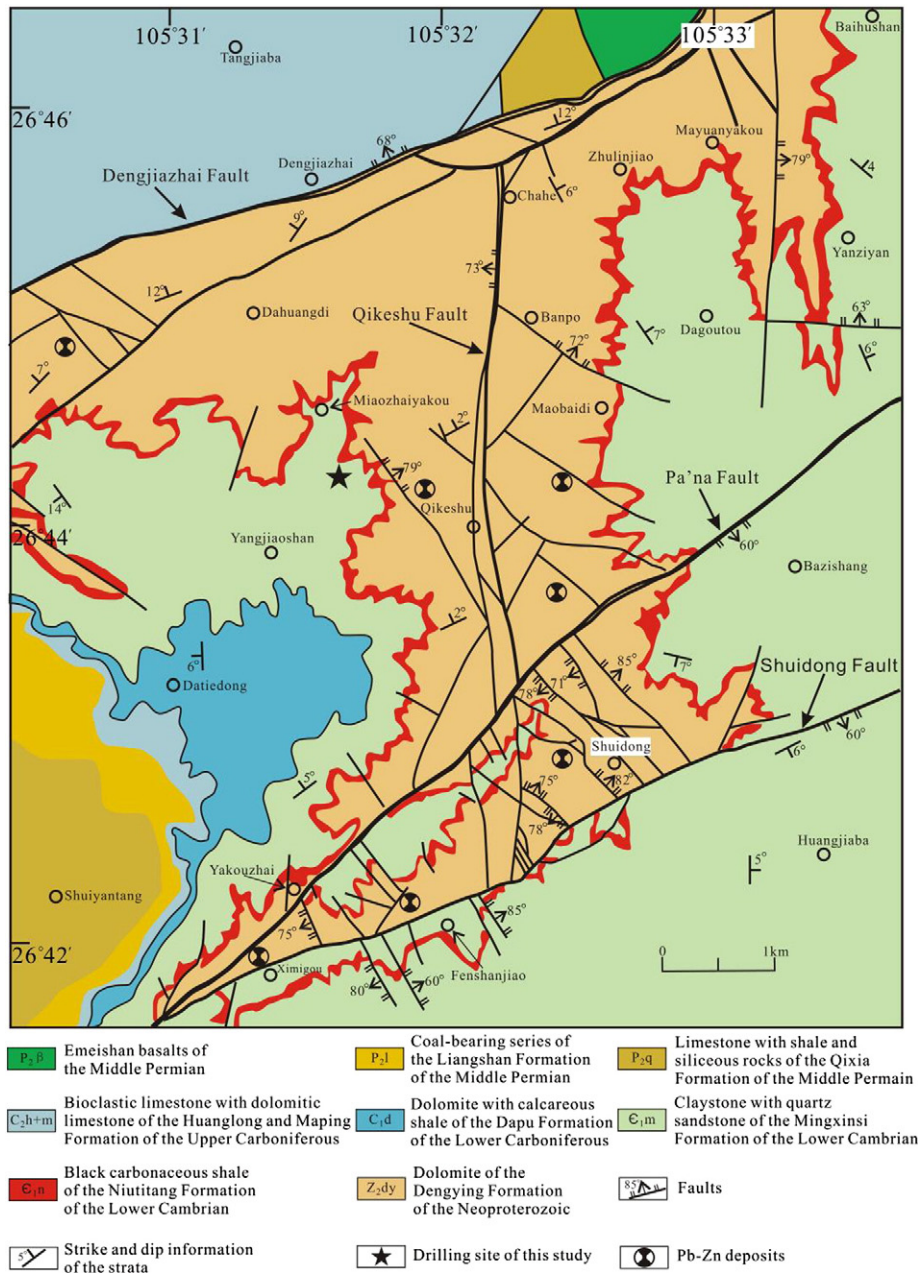


Fig. 2. Geological map of the polymetallic Ni–Mo–PGE mineralization in the black shales of the Lower Cambrian Niutitang Formation in Shuidong, Nayong, Guizhou Province (modified from Wu and Xu, 2010).

(Mo, Fe, Ni)<sub>3</sub>(S, As)<sub>6</sub>C<sub>10</sub> (Kao et al., 2001), is the only Mo-bearing phase and usually occurs as clasts and bands (Fig. 4e, f). The abundant sphalerite in the ores of Nayong area differs from those of Zunyi and Zhangjiajie. Sphalerite and millerite occur in association with pyrite and MoSC in the clasts, whereas in other instances they infill fractures in the MoSC phase (Fig. 4e, f). However, in the polymetallic ores of the Nayong area, ellipsoidal organic clots with variable Ni and Mo contents (Ni in the inner part and Mo in the outer part), which have recently been reported in the Zunyi deposits (Cao et al., 2013; Shi et al., 2014), are not found. Furthermore, in some samples, the MoSC phase and apatite nodules are often dissected by millerite, sphalerite and barite. This feature suggests that the deposition of Mo and P might precede that of Ni, Zn and Ba (Fig. 4f). Gangue minerals are mainly apatite, barite, calcite, quartz and other silicate minerals. In contrast, sporadic and aggregate pyrite dispersed in the silicate matrix is a common feature in the black shale.

### 3. Samples and methods

Nine samples (eight of black shale and one of polymetallic ore) of the Lower Cambrian Niutitang Formation were collected from drill cores (Table 1, Figs. 2 and 3). Twelve ore samples were collected from the surface in the town of Shuidong, Nayong county. All samples were ground to minus 200 mesh in an agate mortar. Chemical reagents such as hydrofluoric acid (HF, 40 wt.%), hydrochloric acid (HCl, 37 wt.%) and nitric acid (HNO<sub>3</sub>, 69 wt.%), used in the experiments were purified by sub-boiling distillation.

Trace elements in the black shale were determined by a Perkin-Elmer Sciex ELAN DRC-e ICP-MS at the State Key Laboratory of Ore Deposit Geochemistry (SKLODG), Institute of Geochemistry, Chinese Academy of Sciences (Guiyang). A 50 mg powder sample was dissolved in a high-pressure Teflon bomb with 1 ml HF and 2 ml HNO<sub>3</sub> at 190 °C for 48 h. After removing HF by heating, the residue was dissolved in



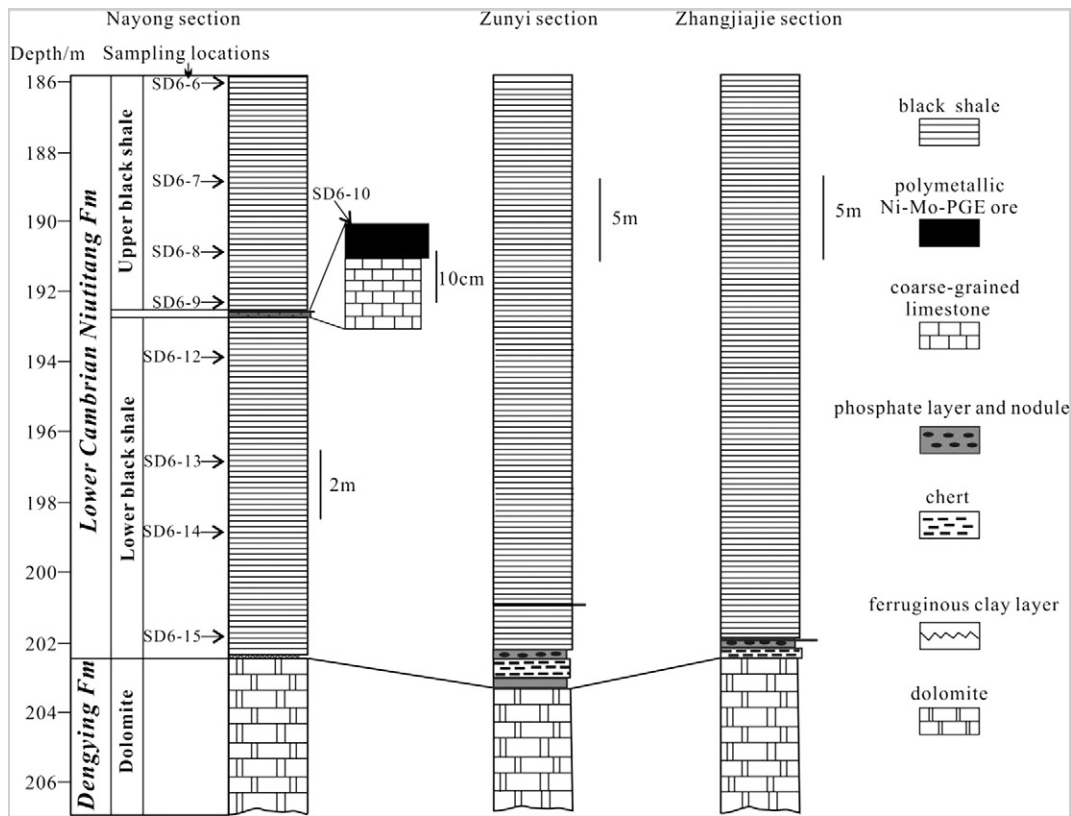


Fig. 3. Lithological column and sampling locations in the drill hole examined in Shuidong, Nayong, Guizhou Province compared to Zunyi (Guizhou Province) and Zhangjiajie (Hunan Province) sections (Zunyi and Zhangjiajie sections modified from Steiner et al., 2001).

2 ml H<sub>2</sub>O and 2 ml HNO<sub>3</sub> with an appropriate amount of Rh at 145 °C for 12 h (Qi et al., 2000). Rh was used as an internal standard to monitor instrumental drift during the analysis: analytical precision was better than 10% relative standard deviation. The polymetallic ores were similarly dissolved and trace elements were determined by a Finnigan MAT ELEMENT high-resolution ICP-MS at the Chinese National Research Center of Geoanalysis (Beijing). Total analytical precision was better than 10% relative standard deviation.

An improved digestion technique with a 120 ml polytetrafluoroethylene (PTFE) beaker and stainless steel pressure bomb was used in the PGE analyses (Qi et al., 2011). Two to three grammes of powder sample was first dissolved in 5 ml HF and 15 ml HNO<sub>3</sub> in a 120 ml PTFE beaker on a hot plate to remove the silicates and sulfides. The dried residue with an appropriate amount of enriched isotope spike solution containing <sup>101</sup>Ru, <sup>193</sup>Ir, <sup>105</sup>Pd and <sup>194</sup>Pt was digested with 5 ml HF and 15 ml HNO<sub>3</sub> in a sealed beaker inside a stainless steel pressure bomb at 190 °C for 48 h, and the solution was evaporated to dryness after dissolution. Then, 5 ml HCl was added to remove the residual HF and HNO<sub>3</sub> from the sample, which was subsequently evaporated to dryness. The final residue was dissolved in 40 ml 2 N HCl and centrifuged. The upper, clear solution was used to pre-concentrate PGE by Te coprecipitation. The main interfering elements, such as Cu, Ni, Zr and Hf, were removed using a mixed ion-exchange column containing a Dowex 50 W X8 cation exchange resin and a P507 Levetrel resin. The eluted solution was measured by the ELAN DRC-e ICP-MS at SKLOGD, and the detection limits ranged from 0.004 ppb Ir to 0.014 ppb Pt (Qi et al., 2011).

Total organic carbon (TOC) was obtained by a Leco CS230 carbon and sulfur analyzer at the ALS Chemex (Guangzhou) Company Limited. The relative standard deviation was better than 5%.

For mineral observation and identification, a JSM-6440LV scanning electron microscope (SEM) with energy dispersive X-ray spectrometer

(EDS, EDAX) was used at the State Key Laboratory of Environmental Geochemistry, Chinese Academy of Sciences (Guiyang).

#### 4. Results

Elemental enrichment characterizes the black shales of the Lower Cambrian Niutitang Formation in the Nayong area, particularly Ni (7.03 wt.%), Mo (8.49 wt.%) and Zn (11.7 wt.%), all of which occur at percent level (Table 2). Most trace-element concentrations in the black shale are essentially constant, whereas they are highly enriched in the polymetallic ores (Table 2, Fig. 5). Similar trace-element concentrations are seen in the Zunyi and Zhangjiajie deposits except that Zn is unusually high in the Nayong area. In general, the polymetallic ores are characterized by higher concentrations of siderophile elements (Co, Ni and Mo), chalcophile elements (Cu, Zn, Cd, Sb, Tl, Pb and Bi) and two lithophile elements (Y, U) compared to those of the black shale host (Table 2). In contrast, the concentrations of most lithophile elements (Li, Be, Sc, V, Cr, Rb, Zr, Nb, Cs, Th, Hf) in the black shale host are higher than those in the polymetallic ores (Table 2).

The enrichment factor (EF), which is the relative abundance of an element in a sample divided by its average abundance in the upper continental crust (UCC, Rudnick and Gao, 2003), is generally used to describe trace-element enrichment (Harris et al., 2013). For polymetallic ores, the EFs of several lithophile elements are less than or around one except for Y and U that have averages of 9 and 109, respectively (Fig. 5). However, most siderophile and chalcophile elements are moderately to strongly enriched. For instance, the EFs for Co, Ni, Mo, Cu, Zn, As, Cd, Sb, Tl, Pb and Bi range from 10 to more than 10,000 in the polymetallic ores (Fig. 5). In the black shale, the concentrations of most lithophile elements have similar concentrations as the UCC, and the EFs are around one except for V, Sn and U, which are 4, 70 and 9, respectively. Furthermore, there is moderate to weak enrichment in a few

siderophile and chalcophile elements, including Ni, Mo, Cu, Zn, As, Cd, Sb and Tl, with EFs ranging from one to several hundreds in the black shale (Fig. 5).

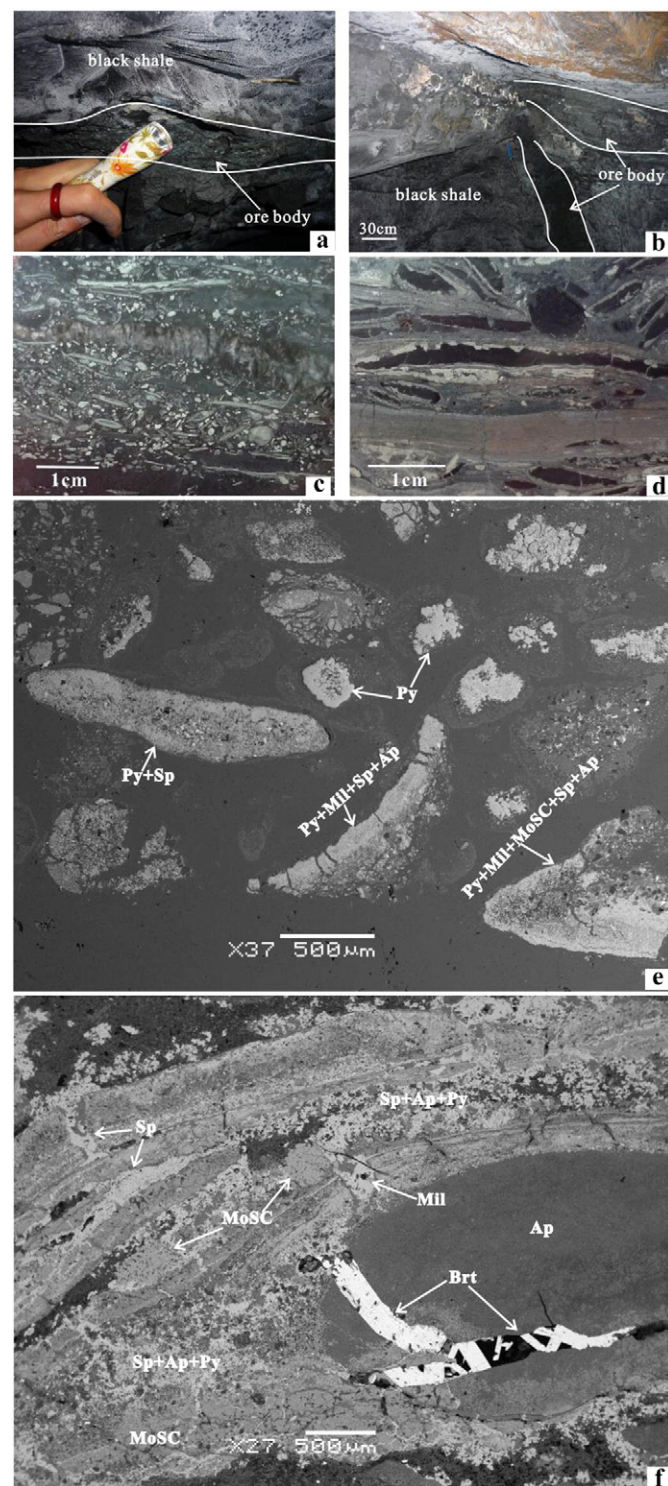


**Fig. 4.** Representative features of the ores and the minerals of the polymetallic mineral systems in Shuidong, Nayong, Guizhou Province. a: horizontal ore body parallel to the hosting strata; b: ore-pipe perpendicular to the flat-lying strata; c: ore sample with lenticular structure and a quartz veinlet; d: ore sample with lenticular and banded structures; e: photomicrograph of Fig. 4c (SEM, BSE,  $\times 27$ ), ore minerals occur as the clasts and nodules and disseminated in silicate matrix; f: photomicrograph of Fig. 4d (SEM, BSE,  $\times 37$ ), ore minerals occur as nodules, clasts and bands, the apatite and MoSC phase are cut by sphalerite, millerite and barite. Abbreviation: Sp: sphalerite, Mil: millerite, Brt: barite, Ap: apatite, Py: pyrite, MoSC: a Mo-bearing phase with admixture of carbonaceous matter and  $\text{MoS}_2$  (Kao et al., 2001; Orberger et al., 2007).

**Table 1**

Sample descriptions of the black shales in the Lower Cambrian Niutitang Formation from a drill hole in Shuidong, Nayong, Guizhou Province.

Sample no.	Sample descriptions
SD6-6	Black shale with laminated structure, sporadic pyrite and fine calcite vein
SD6-7	Black shale with laminated structure, pyrite nodule
SD6-8	Grey to black shale with laminated structure, pyrite nodule, fine pyrite and calcite vein
SD6-9	Pitch black shale with laminated structure closely overlies the polymetallic ore
SD6-10	Pitch black polymetallic Ni-Mo-PGE ore with a highest TOC, banded and lenticular structure
SD6-12	Grey to black shale with laminated structure, pyrite nodule, calcite vein
SD6-13	Grey to black shale with laminated structure, fine pyrite, calcite vein, apatite nodule
SD6-14	Black shale with laminated structure, sporadic pyrite
SD6-15	Black shale with laminated structure, abundant apatite nodule

High TOC is a notable feature for the black shales of the Lower Cambrian Niutitang Formation in the Nayong area. TOC in the polymetallic ores ranges from 2.55 wt.% to 11.5 wt.% with an average of 7.73 wt.%, whereas in the black shale, TOC ranges from 1.80 wt.% to 4.26 wt.% with an average of 3.67 wt.% (Table 2). PGE data are summarized in Table 3. There are large differences between the PGE of the polymetallic ores and the black shale. The highest PGE concentrations are detected in the polymetallic ores with an average of 4.70 ppb for Ru, 9.93 ppb for Rh, 288 ppb for Pd, 2.32 ppb for Ir and 308 ppb for Pt and total PGE concentrations of up to 943 ppb (Table 3). In contrast, the black shale has lower total PGE concentrations and averages of 0.224 ppb for Ru, 0.145 ppb for Rh, 9.16 ppb for Pd, 0.090 ppb for Ir and 3.33 ppb for Pt (Table 3). Pt and Pd are enriched relative to Ru, Rh and Ir in the polymetallic ores and black shale; furthermore, the PGE concentrations, geochemical parameters and chondrite-normalized PGE patterns significantly vary (Table 3, Fig. 6).

As mentioned above, the polymetallic ores are enriched in several elements compared to the black shale host (Tables 2 and 3). Positive correlations among most of enriched trace elements are observed for the polymetallic ores, but are absent in the black shale. Therefore, we divide the enriched elements into three groups according to correlation coefficients ( $R^2$ ) and geochemical properties: Co–Ni–Cu–PGE, Zn–Cd–Pb and Mo–Tl–TOC (Table 4);  $R^2 \geq 0.80$  denotes strong correlation and  $R^2$  between 0.80 and 0.50 denotes moderate correlation (Harris et al., 2013).

In the polymetallic ores, moderate to strong positive correlations are found among Co, Ni and Cu with  $R^2$  values ranging between 0.69 and 0.92, whereas such correlations are not found in the black shale (Table 4). Moreover, Cu and Co show moderately positive correlations with PGE, especially Ru, Pd and Pt with the  $R^2$  values ranging between 0.58 and 0.71, in the polymetallic ores (Table 4). However, Ni does not correlate with PGE in the polymetallic ores.

There is a strong correlation between Zn and Cd ( $R^2 = 0.76$ ) in the polymetallic ores but not in the black shale (Table 4), which is consistent with the tendency of sphalerite to host Cd. However, Pb, which commonly coexists with Zn in the Pb–Zn deposits, shows weak correlation with Zn ( $R^2 = 0.19$ , Table 4).

Mo strongly correlates with Tl in the polymetallic ores ( $R^2 = 0.74$ ) and black shale ( $R^2 = 0.91$ ) (Table 4). In addition, TOC is strongly positively correlated with Mo ( $R^2 = 0.74$ ) and Tl ( $R^2 = 0.80$ ) in the polymetallic ores (Table 4). In particular, Mo and TOC are strongly correlated with PGE in the polymetallic ores with  $R^2$  of 0.56–0.87 for TOC–PGE and 0.52–0.83 for Mo–PGEs except Rh (Table 4).

## 5. Discussion

Despite the extensive research efforts regarding the origin of the polymetallic Ni–Mo–PGE mineralization, the metal sources are yet to be identified with certainty. Coexistence of numerous elements with

**Table 2**

Trace elements concentrations and TOC in the black shales of the Lower Cambrian Niutitang Formation in Shuidong, Nayong, Guizhou Province (TOC is in wt.%, other elements are in ppm).

Sample no.	Lithology	Li	Be	Sc	V	Cr	Co	Ni	Cu	Zn	Ga	Ge	As	Rb	Sr	
SD6-6	Upper	25.8	3.06	14.8	409	90.5	16.9	79.4	58.5	97.1	21.3	1.57	6.67	134	154	
SD6-7	Black	15.3	2.75	14.5	701	105	22.6	281	78.0	317	20.0	1.38	18.1	119	198	
SD6-8	shale	12.1	2.20	10.0	193	79.9	23.4	279	87.3	186	14.9	1.50	210	89.2	87.5	
SD6-9		17.7	2.90	12.6	437	86.5	21.6	869	64.6	619	21.3	1.68	37.1	112	148	
SD6-10	Ore	2.07	0.260	1.32	217	43.5	261	20679	1997	5532	5.46	1.18	10370	11.1	56.8	
SD3-16	sample	10.5	1.19	6.00	204	38.2	316	36194	2628	95774	14.6	11.0	9398	9.02	320	
SD7-1		9.49	1.61	7.81	198	56.9	437	67330	3847	62495	36.2	3.43	14975	17.3	402	
SD7-2		11.8	2.06	12.0	237	50.0	300	38720	2772	66602	26.6	2.50	11605	20.2	426	
SD7-3		3.53	0.400	2.83	61.5	16.6	109	14688	740	12915	15.8	0.830	3340	4.57	298	
SD8-7		6.57	1.13	5.50	105	50.5	137	18050	1116	16842	11.3	2.38	7487	16.9	286	
SD8-8		5.66	0.420	2.96	71.2	25.1	150	21231	1201	10045	12.8	1.10	7047	4.54	306	
SD5-4		7.05	1.02	5.96	152	51.3	275	48284	2530	115515	24.4	14.9	4827	9.85	322	
SD1-6		20.2	1.80	7.08	552	79.9	397	51009	2545	14637	18.7	2.19	18054	23.5	278	
JL-1		6.46	0.960	5.13	151	48.8	409	70292	3314	116712	25.0	12.5	8866	6.90	294	
DJLZ2-1		20.6	0.350	2.50	158	51.7	368	30347	3339	26175	9.07	4.12	8452	9.13	74.1	
DJLZ3-1		13.7	1.11	7.04	163	38.5	180	19942	1484	35800	14.6	7.36	3939	18.3	414	
DJLZ3-2		8.65	1.22	8.42	184	50.5	313	41538	2440	49439	20.9	11.8	8231	13.3	312	
SD6-12	Lower	22.1	2.63	11.6	408	100	16.8	216	45.3	353	16.7	1.33	31.2	93.3	138	
SD6-13	black	25.3	1.61	6.77	354	373	5.34	71.8	58.2	104	10.6	0.995	8.07	53.7	178	
SD6-14	sample	28.4	1.96	10.3	446	87.1	14.7	180	51.1	199	15.2	1.23	21.4	83.1	72.8	
SD6-15		33.6	2.24	8.18	482	538	7.90	102	73.5	141	12.9	1.03	10.2	74.2	139	
Average of black shale		22.5	2.42	11.1	429	183	16.2	260	64.6	252	16.6	1.34	42.9	94.8	139	
Average of ore sample		9.71	1.04	5.73	189	46.3	281	36793	2304	48345	18.1	5.79	8969	12.7	291	
Black shale of ZY and ZJJ <sup>a</sup>				13.1	825	99.2	23.0	394	93.9	531	18.8			107	131	
Ores of ZY and ZJJ <sup>a</sup>				3.56	1240	76.5	146	36000	1370	7460	10.4			31.5	498	
Y	Zr	Nb	Mo	Cd	Sn	Sb	Cs	Ba	Hf	W	Tl	Pb	Bi	Th	U	TOC
28.2	139	12.7	16.7	5.42	139	1.63	17.2	928	4.12	1.81	1.87	48.1	0.382	12.0	14.9	1.80
30.3	142	12.2	64.0	22.2	590	4.67	14.5	1100	4.03	1.71	3.36	46.8	0.454	11.8	26.4	3.04
20.8	96.3	9.10	48.6	4.90	121	10.1	11.6	759	2.76	1.33	4.04	185.0	0.263	8.69	35.4	3.88
23.9	124	11.8	439.1	4.78	22.8	7.51	13.8	842	3.27	2.21	8.92	49.8	0.419	10.8	38.5	5.41
3.51	12.8	0.9	72913	217	6.56	246	12.0	211	0.230	2.77	265	364	6.82	0.330	11.2	11.45
227	19.8	1.20	36643	671	11.5	257	5.12	161	0.410	1.19	186	407	12.0	3.40	424	9.68
375	34.8	2.23	36267	617	19.8	309	5.91	267	0.760	1.12	200	431	20.0	4.46	359	6.94
445	45.6	2.48	31242	559	16.2	272	5.21	288	0.900	1.15	196	414	13.9	5.77	431	7.33
94.6	8.91	0.6	7346	87	3.69	72.3	1.04	2875	0.230	0.500	47.5	137	4.71	1.42	156	2.55
102	30.4	1.84	25647	208	7.72	144	5.97	502	0.690	1.13	110	173	6.20	3.02	219	5.38
90.1	8.23	0.6	17569	139	7.25	160	2.33	259	0.200	0.690	106	197	8.31	1.75	143	3.76
229	22.3	1.26	37492	858	15.1	268	3.45	1041	0.470	1.54	193	376	12.9	3.72	512	9.74
182	70.1	3.16	40082	149	10.4	325	7.60	403	1.30	1.56	186	185	8.70	4.32	373	8.17
263	17.4	0.96	29857	879	14.0	311	2.56	2173	0.400	1.13	161	371	14.1	3.01	520	8.37
61.6	18.0	0.97	84922	523	12.9	564	6.44	1802	0.270	1.96	245	599	17.0	1.24	74.3	11.05
172	35.5	2.01	30714	521	9.01	312	4.04	481	0.670	1.00	99.3	290	10.2	3.34	257	7.08
301	31.5	1.67	49905	828	14.1	446	5.15	634	0.530	1.97	220	382	10.5	3.72	354	8.95
17.1	175	12.8	41.9	8.46	221	4.05	11.00	1070	4.86	1.39	3.34	50.2	0.255	10.0	23.0	3.72
63.7	90.8	7.59	6.11	0.28	2.16	1.02	7.53	665	2.56	1.11	1.05	14.8	0.036	6.13	13.6	3.79
20.6	180	11.5	25.0	3.10	81.3	4.65	10.3	798	4.82	1.21	2.24	44.5	0.170	8.45	26.3	4.26
40.9	118	9.56	7.99	0.53	5.06	1.73	11.1	819	3.42	0.97	1.61	22.1	0.083	7.81	14.9	3.49
30.7	133	10.9	81.2	6.21	148	4.42	12.1	873	3.73	1.47	3.30	57.7	0.258	9.46	24.1	3.67
196	27.3	1.53	38508	481	11.4	284	5.14	854	0.543	1.36	170	333	11.2	3.04	295	7.73
152	11.9	253			2.40	8.83	11.8	1350	3.66	3.88		27.6	0.600	11.3	43.0	
43.1	3.60	53800			5.25	227	7.91	6580	3.05	30.8		95.6	10.9	53.8	252	

<sup>a</sup> Zunyi (ZY) and Zhangjiajie (ZJJ) average values from Xu et al. (2012).

various geochemical properties (mixture of elements associated with felsic, mafic and ultramafic rocks) may be critical for elucidating the unidentified metal sources. Several studies have proposed that metals for the Ni–Mo–PGE mineralization are possibly derived from extraterrestrial materials or mafic and ultramafic rocks (Fan, 1983; Fan et al., 1984; Li and Gao, 2000; Lott et al., 1999). Additional studies have obtained detailed evidence for the sources of the Ni–Mo–PGE mineralization. Jiang et al. (2006) suggested that the terrigenous sources for the high-field-strength elements, such as Zr, Hf, Nb, Ta, Sc, Th, REE, Rb and Ga, and mixing of seawater and hydrothermal vents for V, Ni, Mo, U, Mn, Cu, Zn, Pb, Sr and Ba. Pašava et al. (2010) suggested that felsic tuffs which interbedded with phosphorites have unusual high PGE concentrations at the Kunyang deposit and might be possible source of PGE for the younger Mo–Ni–PGE phosphatic and sulfide-bearing black shales. Recently, it was proposed that metals in the polymetallic ores were mostly

scavenged from Early Cambrian seawater (Xu et al., 2012). In the following discussion, we primarily focus on the metal sources for this type of mineral systems.

### 5.1. Source of Co, Ni, Cu and PGE

#### 5.1.1. Co, Ni and Cu

Co, Ni and Cu are strongly chalcophile elements and typically have higher concentrations in mafic and ultramafic rocks than in felsic and intermediate rocks. They can coexist and be isomorphous with each other because of their similar geochemical properties. Similar to Co, Ni and Cu, PGE are also strongly chalcophile and tend to be enriched in mafic and ultramafic rocks (Liu et al., 1984). The high concentrations and positive correlations of these metals in the polymetallic ores of the Lower Cambrian black shales (Tables 2 and 4) imply that Co, Ni



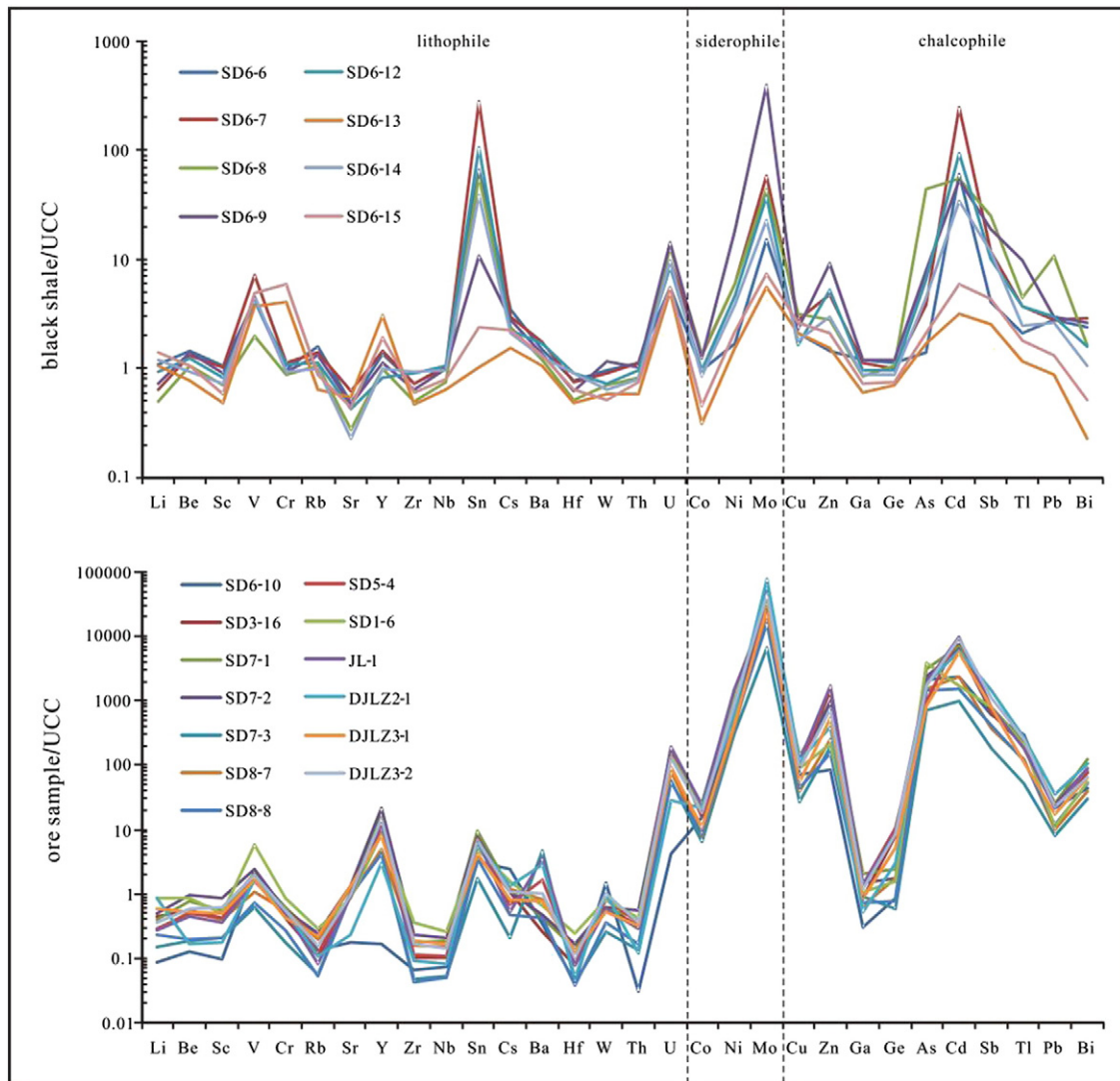


Fig. 5. Spider diagrams and enrichment factors of the trace elements for the black shales of the Lower Cambrian Niutitang Formation in Shuidong, Nayong, Guizhou Province normalized to the upper continental crust (UCC, Rudnick and Gao, 2003).

and Cu may be genetically related with the mafic and ultramafic rocks. On the other hand, trace elements, such as Co, Ni and Cu, often can be associated with hydrothermal fluids that record the interaction between seawater and mafic or ultramafic rocks in a marine environment. For instance, Co, Ni and Cu enrichment is observed in relatively high-temperature, low-pH, and Cl-rich fluids that have undergone phase separation and interacted with ultramafic rocks (Douville et al., 2002; Marques et al., 2006). Co and Ni can be released from peridotite minerals and enter the newly formed serpentine and magnetite or precipitate as Ni–Co–Fe sulfides in the presence of aqueous  $H_2S$  (Marques et al., 2007). These metals can also be leached during the alteration of basaltic rocks. Mottl et al. (1979) concluded that Cu is extensively leached from basalt and andesite because of hydrothermal alteration. Seewald and Seyfried (1990) suggested that fluid chemistry is characterized by high Zn, Cu, Fe, Mn,  $SiO_2$ ,  $H_2S$  and  $H_2$  concentrations during basalt alteration at 400 °C. The concentrations of Fe, Mn and Cu can reach up to 1500, 190 and 0.3 ppm, respectively, during basalt–seawater interaction at 200–500 °C at 500–800 bars (Hajash, 1975). Considering these features, it appears that mafic and ultramafic rocks may be the source of Co, Ni and Cu for the polymetallic ores of the Lower Cambrian black shales. Coincidentally, mafic and ultramafic rocks were widely developed in southern China in the Proterozoic and Early Palaeozoic eras (Li and Gao, 2000). However, the mechanism for the extreme enrichment

of Ni compared to Co and Cu is unclear. A possible reason for this might be that only very small fractions of the Co and Cu metals in hydrothermal fluids are deposited along with Ni. This phenomenon might be similar to that suggested for the Avebury hydrothermal Ni deposit, Tasmania (Keays and Jowitt, 2013).

#### 5.1.2. PGE

PGE are not exclusively associated with mafic and ultramafic rocks because they can also be enriched in the marine environments (Pašava, 1993; Sawlowicz, 1993). Several studies of significant PGE enrichment have been performed to understand the migration and enrichment process of PGE at low temperatures in manganese nodules, ferromanganese crusts and submarine hydrothermal sulfides (Banakar et al., 2007; Crocket, 1990; Li, 1991; Pašava et al., 2004, 2007).

The PGE concentrations of the polymetallic ores in the Nayong area are consistent with those of the Zunyi and Zhangjiajie reported in an earlier study (Table 3, Xu et al., 2012). Furthermore, the black shale has PGE concentrations less than those in the Zunyi and Zhangjiajie areas (Table 3, Xu et al., 2012). In terms of the PGE geochemistry concerning the black shale in Nayong, the chondrite-normalized PGE patterns are similar to those of the upper continental crust (UCC, Park et al., 2012), marine oil shale (Fu et al., 2011) and seawater (Nozaki, 1997) (Fig. 6). On the other hand, the average Pd/Pt value of 2.75 for

**Table 3**  
PGE concentrations in the black shales of the Lower Cambrian Niutitang Formation in Shuidong, Nayong, Guizhou Province (ppb).

Sample no.	Lithology	Ru	Rh	Pd	Ir	Pt	Pd/Pt	Pd/Ir	Pt/Ir	∑ PGE
SD6-6	Upper	0.128	0.097	5.78	0.113	1.81	3.19	51.0	16.0	7.93
SD6-7	black	0.329	0.162	11.2	0.129	4.00	2.80	86.7	30.9	15.8
SD6-8	shale	0.147	0.130	7.07	0.126	3.19	2.22	55.9	25.2	10.7
SD6-9		0.419	0.218	13.3	0.119	7.30	1.82	112	61.3	21.4
SD6-10	Ores	5.14	12.1	374	3.87	350	1.07	96.6	90.4	745
SD3-16		5.28	15.2	333	2.02	381	0.874	165	189	736
SD7-1		5.18	7.44	316	2.49	326	0.969	127	131	657
SD7-2		5.37	9.76	300	1.88	376	0.798	160	200	693
SD7-3		1.87	3.43	100	0.830	103	0.971	120	124	210
SD8-7		2.76	7.25	163	1.40	172	0.948	116	123	347
SD8-8		3.00	6.28	173	1.31	182	0.951	132	139	365
SD5-4		5.79	19.1	360	2.58	430	0.837	140	167	818
SD1-6		6.38	13.2	288	2.04	378	0.762	141	185	688
JL-1		5.10	9.37	340	2.90	306	1.11	117	106	663
DJLZ2-1		6.94	12.8	454	3.80	466	0.974	119.	123	943
DJLZ3-1		3.70	5.45	205	2.03	200	1.03	101	98.5	416
DJLZ3-2		4.64	7.76	344	2.97	331	1.04	116	111	691
SD6-12	Lower	0.128	0.094	4.83	0.072	1.91	2.53	67	26.5	7.04
SD6-13	black	0.219	0.136	10.3	0.045	2.49	4.14	229	55	13.2
SD6-14	shale	0.122	0.112	3.24	0.077	1.80	1.80	41.9	23.3	5.35
SD6-15		0.301	0.212	17.5	0.039	4.16	4.2	444	106	22.2
Average black shale (this study)		0.224	0.145	9.16	0.090	3.33	2.75	102 (60.2) <sup>f</sup>	37.0 (30.6) <sup>f</sup>	13.0
Average ore sample (this study)		4.70	9.93	288	2.32	308	0.94	124	133	613
Black shale of ZY and ZJJ <sup>a</sup>		6.76	1.04	20.0	1.13	37.8	0.529	17.7	33.5	66.7
Ores of ZY and ZJJ <sup>a</sup>		9.81	12.1	328	3.78	315	1.04	86.8	83.3	669
Marine oil shale <sup>b</sup>		0.112	0.083	3.23	0.043	1.60	2.02	75.9	37.6	5.06
UCC <sup>c</sup>		0.030	0.018	0.526	0.022	0.599	0.878	23.9	27.2	1.20
Seawater <sup>d</sup>		<5.0E-06	8.0E-05	6.0E-05	1.30E-07	5.0E-05	1.2	462	385	1.93E-04
MORB <sup>e</sup>		0.067	0.008	0.460	0.030	0.41	1.12	15.33	13.67	0.975
OIB <sup>e</sup>		0.44	0.24	4.60	0.280	4.6	1.02	16.43	15.36	9.86

<sup>a</sup> Zunyi (ZY) and Zhangjiajie (ZJJ) average values from Xu et al. (2012).  
<sup>b</sup> Marine oil shale (MOS) average value from Fu et al. (2011).  
<sup>c</sup> Upper continental crust (UCC) value from Park et al. (2012).  
<sup>d</sup> Seawater value from Nozaki (1997) and half value of Ru is used for calculation.  
<sup>e</sup> Mid-ocean ridge basalt (MORB) and ocean-island basalt (OIB) values from Crocket (2002).  
<sup>f</sup> Data in parentheses are the average values for black shale excluding two apatite-bearing black shale SD6-13 and SD6-15.

the black shale is very close to that of marine oil shale (Pd/Pt = 2.02) (Table 3). Moreover, this value is relatively higher than that of UCC (Pd/Pt = 0.88) and seawater (Pd/Pt = 1.2) (Table 3). The average Pd/Ir and Pt/Ir values of 69.2 and 30.6, respectively, except for two apatite-bearing black shale (SD6-13 and SD6-15), are also similar to that of marine oil shale (Pd/Ir = 75.9 and Pt/Ir = 37.6) (Table 3). However, the Pd/Ir and Pt/Ir values of the black shale are between those of UCC (Pd/Ir = 23.9 and Pt/Ir = 27.2) and seawater (Pd/Ir = 462 and

Pt/Ir = 385) (Table 3). The similarities with marine oil shale and the discussed above suggest that the black shale may have undergone similar PGE enrichment processes like the marine oil shale that formed in a normal marine sedimentary environment (Fu et al., 2011). Mixtures of seawater and terrigenous materials are possible sources for the black shale of the Lower Cambrian Niutitang Formation.

In contrast to the black shale, the polymetallic ores show higher PGE enrichment than that of the black shale and seafloor hydrothermal

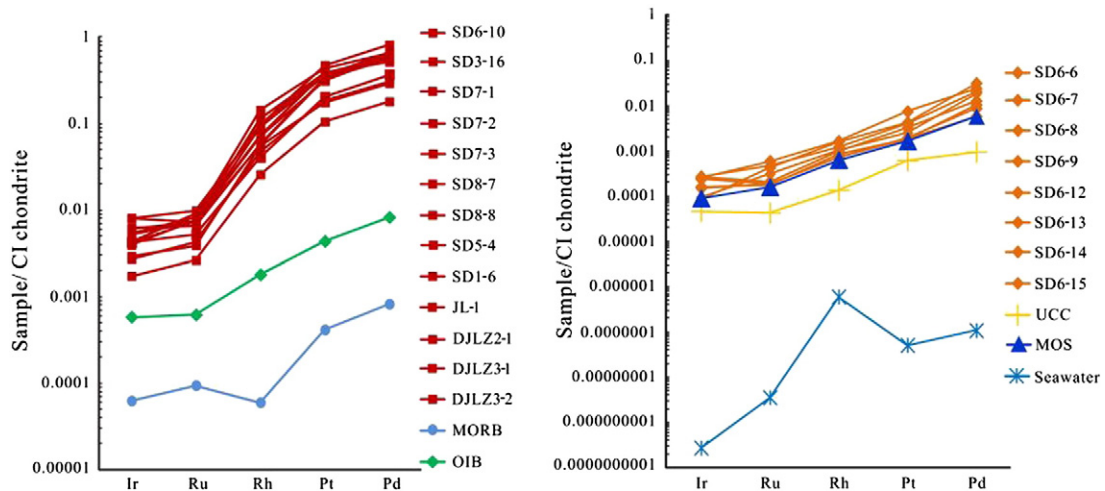


**Fig. 6.** Chondrite normalized PGE patterns for the polymetallic Ni-Mo-PGE ores (left) and the black shale (right) in Shuidong, Nayong, Guizhou Province. CI chondrite value from Anders and Gressge (1989), other values from Table 3. Mid-ocean ridge basalt (MORB) and ocean-island basalt (OIB) values from Crocket (2002); Upper continental crust (UCC) value from Park et al. (2012); Marine oil shale (MOS) average value from Fu et al. (2011); Seawater value from Nozaki (1997) and half value of Ru is used for calculation.



**Table 4**  
Correlation matrix for the correlation coefficient  $R^2$  of the enriched elements in the polymetallic Ni–Mo–PGE ores (a) and black shale (b) of the Lower Cambrian Niutitang Formation in Shuidong, Nayong, Guizhou Province.

	Co	Ni	Cu	Zn	Mo	Cd	Tl	Pb	Ru	Pd	Ir	Pt	Rh	TOC
<i>a</i>														
Co	1.00													
Ni	0.74	1.00												
Cu	0.92	0.69	1.00											
Zn	0.22	0.46	0.32	1.00										
Mo	0.23	0.00	0.24	0.01	1.00									
Cd	0.30	0.41	0.43	0.76	0.04	1.00								
Tl	0.49	0.15	0.51	0.04	0.74	0.16	1.00							
Pb	0.41	0.14	0.63	0.19	0.52	0.43	0.58	1.00						
Ru	0.71	0.32	0.69	0.14	0.52	0.22	0.71	0.54	1.00					
Pd	0.59	0.24	0.66	0.17	0.70	0.36	0.86	0.77	0.83	1.00				
Ir	0.36	0.10	0.39	0.03	0.83	0.20	0.75	0.59	0.52	0.81	1.00			
Pt	0.58	0.25	0.62	0.19	0.52	0.28	0.78	0.62	0.94	0.87	0.52	1.00		
Rh	0.21	0.11	0.22	0.24	0.23	0.15	0.40	0.21	0.58	0.49	0.22	0.69	1.00	
TOC	0.38	0.09	0.39	0.11	0.74	0.26	0.80	0.56	0.71	0.87	0.79	0.75	0.56	1.00
<i>b</i>														
Co	1.00													
Ni	0.32	1.00												
Cu	0.14	0.02	1.00											
Zn	0.30	0.87	0.00	1.00										
Mo	0.20	0.96	0.00	0.81	1.00									
Cd	0.38	0.02	0.06	0.09	0.00	1.00								
Tl	0.42	0.98	0.03	0.86	0.91	0.03	1.00							
Pb	0.40	0.02	0.34	0.00	0.00	0.00	0.06	1.00						
Ru	0.03	0.04	0.20	0.07	0.10	0.01	0.04	0.13	1.00					
Pd	0.05	0.13	0.23	0.07	0.16	0.01	0.08	0.07	0.00	1.00				
Ir	0.26	0.67	0.05	0.63	0.60	0.00	0.67	0.05	0.00	0.02	1.00			
Pt	0.11	0.81	0.13	0.62	0.82	0.00	0.73	0.00	0.02	0.53	0.28	1.00		
Rh	0.03	0.17	0.17	0.11	0.21	0.01	0.11	0.09	0.00	0.91	0.00	0.56	1.00	
TOC	0.01	0.52	0.00	0.46	0.47	0.06	0.45	0.01	0.00	0.10	0.63	0.44	0.12	1.00

sulfides (Table 3, Pašava et al., 2004, 2007). The shape of the chondrite-normalized PGE patterns of the polymetallic ores differs from that of the black shale; however it is typical of mid-ocean-ridge basalt (MORB) and ocean-island basalt (OIB) (Crocket, 2002) (Fig. 6). The Pd/Pt values (average Pd/Pt = 0.94) are almost identical with MORB (Pd/Pt = 1.12) and OIB (Pd/Pt = 1.07) (Table 3). However, there are significant fractionations between PPGE and IPGE. For instance, the Pd/Ir (average Pd/Ir = 124) and Pt/Ir values (average Pt/Ir = 133) of the polymetallic ores are higher than those in MORB (Pd/Ir = 15.33, Pt/Ir = 13.67) and OIB (Pd/Ir = 16.43, Pt/Ir = 15.36) (Table 3). The Pd/Ir and Pt/Ir values are also identical to those in Cu-rich massive sulfides in seafloor hydrothermal systems (Pd/Ir = 114, Pt/Ir = 142, Pašava et al., 2007). The fractionations between PPGE and IPGE are attributed to hydrothermal sulfide deposition where Pt and Pd are more mobile compared to Ir (Maier and Barnes, 1999). Moreover, the Pd/Pt values are identical with those in basalts (MORB and OIB) because the solubility of Pt, either as chloride or bisulfide complexes, is relatively greater than or nearly equal to that of Pd (Wood, 2002). These results suggest that the PGE enrichment in the polymetallic ores could be linked to mafic rocks via hydrothermal processes, which is consistent with Co, Ni and Cu.

### 5.2. Source of Zn, Cd and Pb

Zn and Pb are chalcophile elements, and sphalerite coexists with galena in hydrothermally derived deposits associated with carbonates. Cadmium, another chalcophile element, has similar geochemical behaviour as Zn and is mostly hosted in sphalerite (Bethke and Borton, 1971; Cook et al., 2009). In the black shales of the Lower Cambrian Niutitang Formation in the Nayong area, the polymetallic ores show significantly high Zn concentrations ranging from 0.55 wt.% to 11.7 wt.% and an average of 4.83 wt.%. These values are similar to those in Maluhe, Zhijin area (1.28 wt.% to 2.92 wt.%) (Xu et al., 2012) and Deze, Yunnan province (3.73 wt.%) (Chen et al., 1982) near Nayong, but higher than those in Zunyi (3000 ppm to 5000 ppm) and Zhangjiajie areas (145 ppm to 5000 ppm) (Xu et al., 2012).

Up till now, few studies have investigated the source of Zn, Pb and Cd in the polymetallic Ni–Mo–PGE ore bodies in the black shales of the Lower Cambrian Niutitang Formation, South China. Among the polymetallic ores in the Nayong area, Zn, Pb and Cd do not correlate well with Co–Ni–Cu–PGE and Mo–Tl–TOC (Table 4), especially with the mafic elements and TOC. This suggests that Zn, Pb and Cd may not be genetically related to mafic or ultramafic rocks or organic matter in seawater. Despite this, the Zn, Pb and Cd could have originated from the widespread dolomites underlying the Lower Cambrian black shales. First, because Zn, Pb and Cd could have been leached by hydrothermal fluids flowing through the dolomites and contributed to the above-mentioned acidic, high Cl-rich and high-temperature hydrothermal fluids (Barrett and Anderson, 1988; Wood et al., 1987). In addition, it is well known that the dolomites have high background values of Zn, Pb and Cd and host Pb–Zn deposits. Second, Zn enrichment that reaches up to 11.7 wt.% is an extremely atypical feature of the polymetallic ores in Nayong and its nearby areas because it is not found in Zunyi and Zhangjiajie. Although there are claims that either seawater or mafic and ultramafic rocks can provide metals for the formation of the polymetallic ores (Li and Gao, 2000; Xu et al., 2012), it is difficult to explain the extreme Zn enrichment in the Nayong area and its absence in Zunyi and Zhangjiajie. The difference between the Nayong, Zunyi and Zhangjiajie mineral deposits is the occurrence of Pb–Zn deposit in the dolomites of the Neoproterozoic Dengying Formation in Nayong, which might explain high Zn concentration in the polymetallic ores of the Nayong. Furthermore, the hydrothermal leaching of mafic and ultramafic rocks may contribute to Zn enrichment, as it does for Co, Ni and Cu (Seewald and Seyfried, 1990; Marques et al., 2007). Nevertheless, the high Zn concentration in the polymetallic ores in Nayong is more likely attributed to the underlying Pb–Zn deposits in the dolomites. Third, hydrothermal quartz and calcite veins found in the mining areas carrying minor amounts of ore and gangue minerals, such as barite, sphalerite, pyrite, chalcophyllite and fluorite, often cut through the mineralized shales and Neoproterozoic dolomites (Lott et al., 1999; Orberger et al., 2007). The veins and ore minerals also indicate that the Zn could have

been extracted from the underlying dolomites by the hydrothermal processes.

However, the correlation between Zn and Pb is weak ( $R^2 = 0.19$ ) compared to that of Zn and Cd ( $R^2 = 0.76$ ) in the polymetallic ores (Table 4), which possibly results from the different solubility of sphalerite and galena in the hydrothermal conditions. For instance, ZnS is consistently more soluble than PbS in acidic, Cl-rich and high-temperature hydrothermal processes (Barrett and Anderson, 1988; Wood et al., 1987).

The Zn anomaly and the Pb–Zn deposits, as well as correlations, suggest that the dolomites and/or Pb–Zn deposits of the Neoproterozoic Dengying Formation, rather than seawater or mafic and ultramafic rocks, could be the main source of Zn, Pb and Cd by hydrothermal leaching.

### 5.3. Source of Mo, Tl and TOC

Molybdenum is widely used as a palaeoredox indicator (Chappaz et al., 2014; Orberger et al., 2007; Scott and Loyns, 2012; Tribouillard et al., 2012). It is known that Mo is typically present as stable and unreactive molybdate anion ( $\text{MoO}_4^{2-}$ ) in the seawater and the enrichment of authigenic Mo is limited in oxic conditions (Algeo and Tribouillard, 2009; Tribouillard et al., 2006). Conversely, molybdenum can be reduced to particle-reactive thiomolybdate ions ( $\text{MoO}_x\text{S}_4^{2-x}$ ) or tetrathiomolybdate ( $\text{MoS}_4^{2-}$ ) in the presence of  $\text{H}_2\text{S}$  under anoxic conditions, and is thus rapidly fixed in sediments (Erickson and Helz, 2000; Helz et al., 1996, 2011). In addition, in the black shales of the Lower Cambrian in southern China, organic matter is mostly derived from marine algae, plankton and benthic communities (Chen et al., 2006; Křibek et al., 2007; Wu et al., 1999). This organic matter can commonly collect as a variety of forms such as separate accumulations, veinlets and small pellets in the matrix and phosphatised or sulfidised clasts in the polymetallic ores (Křibek et al., 2007; Pašava et al., 2008). In fact, organic matter plays a crucial role in sourcing, transporting and precipitating numerous elements in sedimentary environments through complex formation between metals and functional groups. (Coveney and Pašava, 2004; Mostofa et al., 2013).

In the polymetallic ores, there is strong correlation between Mo and organic matter. First, the abundant Mo-bearing phases in the polymetallic ores are a mixture of carbonaceous matter and  $\text{MoS}_2$  at the nanoscale (Kao et al., 2001; Orberger et al., 2007). Second, ellipsoidal mineralization-related organic clots (rhodophyte cystocarps) are found in the ores but not in the nearby black shale. Organic clots commonly have high Mo content in the outer part and Ni in the inner part of the rhodophyte cystocarp, which also suggests a significant biotic effect on the polymetallic mineralization (Cao et al., 2013; Shi et al., 2014). Third, there is strong correlation between Mo and TOC ( $R^2 = 0.74$ , Table 4) in the ores. Such strong correlation is often observed in modern and ancient euxinic basins (Chappaz et al., 2014). The above-mentioned observations suggest that Mo may be primarily controlled by functional groups bound with organic matter from seawater (Mostofa et al., 2013). However, the extreme Mo enrichment in the polymetallic ores might be attributed to the abundant nitrogen fixing and Mo-dependent hyperthermophilic or mesophilic bacterial consortia (Orberger et al., 2007).

Similar to Mo, high Tl concentration (up to several hundred ppm) is also observed in the Lower Cambrian black shales, especially in the studied ores and showing strong correlation ( $R^2 = 0.79$ ) between Tl and TOC (Table 4). Moreover, Tl also shows biological affinities that can be seen in several Tl deposits of south-western China such as those Lanmuchang (Guizhou Province) and Nanhua (Yunnan Province). These Tl deposits were subjected to a syngenetic bioenrichment via the metabolism of living organisms (Zhang et al., 2007). Consequently, the extreme Tl concentration in the polymetallic ores of the Lower Cambrian black shales might be attributed to organic matter and bioaccumulation.

In particular, the strong correlations between the main components, such as Mo and TOC, with PGE (Table 4) can be explained by the higher PGE contents may be hosted in these Mo-bearing phase or organic matter in Nayong. This distribution patterns probably provide a further insight into the mode of occurrence of PGE. In the Zunyi and Zhangjiajie areas, the PGE are typically present in several minerals. For instance, Zhang et al. (2005) showed that Pt is highly enriched in micrometre-sized As- and Fe-bearing vaesite, whereas Pd is mainly enriched in a phase similar to MoSC. Orberger et al. (2007) showed that Pd could reach up to 982 ppm and 111 ppm in MoSC and Ni–Fe sulfides, whereas Pt can reach up to 124 ppm and 122 ppm in pyrite and Ni–Fe sulfides, respectively. Recently, Pašava et al. (2013) reported that the main PGE carriers are grainy pyrite and Ni sulfides (up to 490 ppm Pt, 390 ppm Pd and 220 ppm Rh), millerite (up to 530 ppm Pt, 430 ppm Pd and 190 ppm Rh) and gersdorffite (up to 410 ppm). Because of the high PGE concentration which can be considered as an unconventional resource, a detailed in situ investigation of the PGE-carrying minerals with higher resolution and sensitivity is necessary.

Therefore, the above-mentioned data suggest that Mo and Tl enrichment might be attributed to bioaccumulation and have seawater origins. As such organic matter plays an important role in Mo, Tl and PGE in the anoxic sedimentary conditions of the Lower Cambrian black shales in South China.

## 6. Conclusions

The results of our investigation are summarized below:

- (1) The polymetallic Ni–Mo–PGE ores are characterized by higher concentrations of trace elements, PGE and TOC than those of the nearby black shale. The percent grades of Zn in the ores of Nayong area are a distinctive feature not observed in Zunyi and Zhangjiajie.
- (2) The sources of PGE in the polymetallic Ni–Mo–PGE ores and black shale are not the same. The formation of former could involve the mafic rocks and hydrothermal processes, whereas the latter might have had terrigenous and seawater contributions.
- (3) Proterozoic and Early Palaeozoic mafic and ultramafic rocks, dolomites and/or Pb–Zn deposits of the Neoproterozoic Dengying Formation and seawater with hydrothermal and biological processes might have contributed to the polymetallic Ni–Mo–PGE mineralization in the black shales of the Lower Cambrian Niutiang Formation, South China.

## Acknowledgements

Many thanks to Professors Liang Qi (Institute of Geochemistry, CAS), Wenjun Qu (Chinese National Research Center of Geoanalysis) and Assistant engineer Yifan Yin (Institute of Geochemistry, CAS) for their kind help during determination of trace elements and PGE. We thank Professor Raymond M. Coveney Jr. (Department of Geosciences, UMKC) and Professor Khan M. G. Mostofa (Institute of Geochemistry, CAS) for their revisions on the early version of this paper. Many thanks also to Professors Franco Pirajno, Jingwen Mao and two anonymous reviewers for their constructive suggestions and revisions for improving this paper. This work was jointly supported by the National Natural Science Foundation of China (Nos. 41303039) and Guizhou Science and Technology Fund ([2013]2283).

## References

- Algeo, T.J., Tribouillard, N., 2009. Environmental analysis of paleoceanographic systems based on molybdenum–uranium covariation. *Chem. Geol.* 268, 211–225.
- Anders, E., Grevesse, N., 1989. Abundances of the elements: meteoritic and solar. *Geochim. Cosmochim. Acta* 53, 197–214.

- Banakar, V.K., Hein, J.R., Rajani, R.P., Chodamkar, A.R., 2007. Platinum group elements and gold in ferromanganese crusts from Afanasiy-Nikitin seamount, equatorial Indian Ocean: sources and fractionation. *J. Earth Syst. Sci.* 116, 3–13.
- Barrett, T.J., Anderson, G.M., 1988. The solubility of sphalerite and galena in 1–5 m NaCl solutions to 300 °C. *Geochim. Cosmochim. Acta* 52, 813–820.
- Bethke, P.M., Borton Jr., P.B., 1971. Distribution of some minor elements between coexisting sulphide minerals. *Econ. Geol.* 66, 140–163.
- Blundell, D.J., Karnkowski, P.H., Alderton, D.H.M., Oszczepalski, S., Kucha, H., 2003. Copper mineralization of the Polish Kupferschiefer: a proposed basement fault-fracture system of fluid flow. *Econ. Geol.* 98, 1487–1495.
- Cao, J., Hu, K., Zhou, J., Shi, C.H., Bian, L.Z., Yao, S.P., 2013. Organic clots and their differential accumulation of Ni and Mo within early Cambrian black-shale-hosted polymetallic Ni–Mo deposits, Zunyi, South China. *J. Asian Earth Sci.* 62, 531–536.
- Chappaz, A., Lyons, T.W., Gregory, D.D., Reinhard, C.T., Gill, B.C., Li, C., Large, R.R., 2014. Does pyrite act as an important host for molybdenum in modern and ancient euxinic sediments? *Geochim. Cosmochim. Acta* 126, 112–122.
- Chen, N.S., Yang, X.Z., Liu, D.H., Xiao, X.J., Fan, D.L., Wang, L.F., 1982. Lower Cambrian black argillaceous and arenaceous rock series in south China and its associated stratiform deposits. *Miner. Depos.* 2, 39–51 (in Chinese with English abstract).
- Chen, L., Zhong, H., Hu, R.Z., Xiao, J.F., Zou, Y.R., 2006. Early Cambrian oceanic anoxic event in northern Guizhou: biomarkers and organic carbon isotope. *Acta Petrol. Sin.* 22, 2413–2423.
- Cook, N.J., Ciobanu, C.L., Pring, A., Skinner, W., Danyushevsky, L., Shimizu, M., Saini-Eidukat, B., Melcher, F., 2009. Trace and minor elements in sphalerite: a LA-ICP-MS study. *Geochim. Cosmochim. Acta* 73, 4761–4791.
- Coveney Jr., R.M., 2003. Re–Os dating of polymetallic Ni–Mo–PGE–Au mineralization in Lower Cambrian black shales of south China and its geological significance—a discussion. *Econ. Geol.* 98, 661–665.
- Coveney Jr., R.M., Chen, N.S., 1991. Ni–Mo–PGE–Au-rich ores in Chinese black shales and speculations on possible analogues in the United States. *Miner. Depos.* 26, 83–88.
- Coveney Jr., R.M., Pašava, J., 2004. Diverse connections between ores and organic matter. *Ore Geol. Rev.* 24, 1–5.
- Coveney Jr., R.M., Murowchick, J.B., Grauch, R.L., Glascock, M.D., 1992. Gold and platinum in shales with evidence against extraterrestrial sources of metals. *Chem. Geol.* 99, 101–114.
- Crocket, J.H., 1990. Noble metals in seafloor hydrothermal mineralization from the Juan de Fuca and mid-Atlantic ridges: a fractionation of gold from platinum metals in hydrothermal fluids. *Can. Mineral.* 28, 639–648.
- Crocket, J.H., 2002. Platinum-group element geochemistry of mafic and ultramafic rocks. In: Cabri, L.J. (Ed.), *The Geology, Geochemistry, Mineralogy and Mineral Beneficiation of Platinum-Group Elements*. Canadian Institute of Mining, Metallurgy and Petroleum, Spec. vol. 54, pp. 177–210.
- Distler, V.V., Yudovskaya, M.A., Mitrofanov, G.L., Prokof'ev, V.Y., Lishnevskii, E.N., 2004. Geology, composition, and genesis of the Sukhoi Log noble metals deposit, Russia. *Ore Geol. Rev.* 24, 7–44.
- Douville, E., Charlou, J.L., Oelkers, E.H., Bienvenu, P., Jove Colon, C.F., Donval, J.P., Fouquet, Y., Prieur, D., Appriou, P., 2002. The rainbow vent fluids (36°14'N, MAR): the influence of ultramafic rocks and phase separation on trace metal content in Mid-Atlantic Ridge hydrothermal fluids. *Chem. Geol.* 184, 37–48.
- Erickson, B.E., Helz, G.R., 2000. Molybdenum (VI) speciation in sulfidic waters: stability and lability of thiomolybdates. *Geochim. Cosmochim. Acta* 64, 1149–1158.
- Fan, D.L., 1983. Polyelements in the Lower Cambrian black shale series in southern China. In: Augustithis, S.S. (Ed.), *The Significance of Trace Elements in Solving Petrogenetic Problems and Controversies*. Theophrastus Publications S. A, Athens, pp. 447–474.
- Fan, D.L., Yang, R.Y., Huang, Z.X., 1984. The Lower Cambrian black shale series and iridium anomaly in south China. *Developments in Geoscience, 27th International Geological Congress*. Beijing Science Press, Moscow, pp. 215–224.
- Fan, D.L., Ye, J., Yang, R.Y., Huang, Z.X., 1987. The geological events and ore mineralization nearby the Precambrian–Cambrian boundary in Yangtze platform. *Acta Sedimentol. Sin.* 3, 81–96 (in Chinese with English abstract).
- Feng, Z.Z., Peng, Y.M., Jin, Z.K., Bao, Z.D., 2002. Lithofacies palaeogeography of the early Cambrian in China. *J. Palaeogeogr.* 4, 1–14 (in Chinese with English abstract).
- Fu, X.G., Wang, J., Zeng, Y.H., Tan, F.W., Feng, X.L., Chen, W.B., 2011. Geochemistry of platinum group elements in marine oil shale from the Changshe Mountain area (China): implications for modes of occurrence and origins. *Int. J. Coal Geol.* 86, 169–176.
- Gao, Z.M., Li, S.R., 1998. Migration of precious metal at low temperature in black shales of Lower Cambrian, Guizhou and Hunan provinces. In: Tu, G.Z. (Ed.), *Lower Temperature Geochemistry*. Science Press, Beijing, pp. 76–92.
- Hajash, A., 1975. Hydrothermal processes along mid-ocean ridges: an experimental investigation. *Contrib. Mineral. Petrol.* 53, 205–226.
- Harris, N.B., Mnich, C.A., Selby, D., Korn, D., 2013. Minor and trace element and Re–Os chemistry of the Upper Devonian Woodford Shale, Permian Basin, west Texas: insights into metal abundance and basin processes. *Chem. Geol.* 356, 76–93.
- Helz, G.R., Miller, C.V., Charnock, J.M., Mosselmans, J.F.W., Patrick, R.A.D., Garner, C.D., Vaughan, D.J., 1996. Mechanism of molybdenum removal from the sea and its concentration in black shales: EXAFS evidence. *Geochim. Cosmochim. Acta* 60, 3631–3642.
- Helz, G.R., Bura-Nakič, E., Mikac, N., Ciglenečnik, I., 2011. New model for molybdenum behavior in euxinic waters. *Chem. Geol.* 284, 323–332.
- Jiang, S.Y., Tang, J.H., Ling, H.F., Feng, H.Z., Chen, Y.Q., Chen, J.H., 2003. Re–Os isotopes and PGE geochemistry of black shales and intercalated Ni–Mo polymetallic sulfide bed from the Lower Cambrian Niutitang Formation, South China. *Prog. Nat. Sci.* 13, 788–794.
- Jiang, S.Y., Chen, Y.Q., Ling, H.F., Yang, J.H., Feng, H.Z., Ni, P., 2006. Trace- and rare-earth-element geochemistry and Pb–Pb dating of black shales and intercalated Ni–Mo–PGE–Au sulfide ores in lower Cambrian strata, Yangtze Platform, South China. *Miner. Depos.* 41, 453–467.
- Jiang, S.Y., Yang, J.H., Ling, H.F., Chen, Y.Q., Feng, H.Z., Zhao, K.D., Ni, P., 2007. Extreme enrichment of polymetallic Ni–Mo–PGE–Au in lower Cambrian black shales of South China: an Os isotope and PGE geochemical investigation. *Palaeogeogr. Palaeoclimatol. Palaeoecol.* 254, 217–228.
- Kao, L.S., Peacor, D.R., Coveney Jr., R.M., Zhao, G.M., Dungey, K.E., Curtis, M.D., Penner-Hahn, J.E., 2001. A C/MoS<sub>2</sub> mixed-layer phase (MoSC) occurring in metalliferous black shales from southern China, and new data on jordisite. *Am. Mineral.* 86, 852–861.
- Keays, R.R., Jowitt, S.M., 2013. The Aveybury Ni deposit, Tasmania: a case study of an unconventional nickel deposit. *Ore Geol. Rev.* 52, 4–17.
- Křibek, B., Šýkorová, I., Pašava, J., Machovič, V., 2007. Organic geochemistry and petrology of barren and Mo–Ni–PGE mineralized marine black shales of the Lower Cambrian Niutitang Formation (South China). *Int. J. Coal Geol.* 72, 240–256.
- Lehmann, B., Nagler, T.F., Holland, H.D., Wille, M., Mao, J.W., Pan, J.Y., Ma, D.S., Dulski, P., 2007. Highly metalliferous carbonaceous shale and Early Cambrian seawater. *Geology* 35, 403–406.
- Li, Y.R., 1991. Distribution patterns of the elements in the ocean: a synthesis. *Geochim. Cosmochim. Acta* 55, 3223–3240.
- Li, S.R., Gao, Z.M., 2000. Source tracing of noble metal elements in Lower Cambrian black rock series of Guizhou-Hunan Provinces, China. *Sci. China Earth Sci.* 43, 625–632.
- Li, S.R., Xiao, Q.Y., Shen, J.F., Sun, L., Liu, B., Yan, B.K., Jiang, Y.H., 2003. Rhenium-osmium isotope constraints on the age and source of the platinum mineralization in the Lower Cambrian black rock series of Hunan-Guizhou provinces, China. *Sci. China Earth Sci.* 46, 919–927.
- Liu, Y.J., Cao, L.M., Li, Z.L., Wang, H.N., Chu, T.Q., Zhang, J.R., 1984. Geochemistry of the Elements. Science Press, Beijing, pp. 101–398 (in Chinese).
- Lott, D.A., Coveney Jr., R.M., Murowchick, J.B., Grauch, R.L., 1999. Sedimentary exhalative nickel–molybdenum ores in South China. *Econ. Geol.* 94, 1051–1066.
- Loukola-Ruskeeniemi, K., Lahtinen, H., 2013. Multiphase evolution in the black-shale-hosted Ni–Cu–Zn–Co deposit at Talvivaara, Finland. *Ore Geol. Rev.* 52, 85–99.
- Maier, W.D., Barnes, S.J., 1999. The origin of Cu sulfide deposits in the Curaca Valley, Bahia, Brazil: evidence from Cu, Ni, Se, and platinum-group element concentrations. *Econ. Geol.* 94, 165–183.
- Mao, J.W., Lehmann, B., Du, A.D., Zhang, G.D., Ma, D.S., Wang, Y.T., Zeng, M.G., Kerrich, R., 2002. Re–Os dating of polymetallic Ni–Mo–PGE–Au mineralization in lower Cambrian black shales of south China and its geologic significance. *Econ. Geol.* 97, 1051–1061.
- Marques, A.F.A., Barriga, F.J.A.S., Chavagnac, V., Fouquet, Y., 2006. Mineralogy, geochemistry, and Nd isotope composition of the Rainbow hydrothermal field, Mid-Atlantic Ridge. *Miner. Depos.* 41, 52–67.
- Marques, A.F.A., Barriga, F.J.A.S., Scott, S.D., 2007. Sulfide mineralization in an ultramafic-rock-hosted seafloor hydrothermal system: from serpentinization to the formation of Cu–Zn–(Co)-rich massive sulfides. *Mar. Geol.* 245, 20–39.
- Mostofa, K.M.G., Liu, C.Q., Feng, X.B., Yoshioka, T., Vione, D., Pan, X.L., Wu, F.C., 2013. Biogeochemical complexation of dissolved organic matter with trace elements in natural waters. In: Mostofa, K.M.G., Yoshioka, T., Mottaleb, A., Vione, D. (Eds.), *Photobiogeochemistry of Organic Matter: Principles and Practices in Water Environments*. Springer, New York, pp. 769–849.
- Mottl, M.J., Holland, H.D., Corr, R.F., 1979. Chemical exchange during hydrothermal alteration of basalt by seawater-II. Experimental results for Fe, Mn, and sulfur species. *Geochim. Cosmochim. Acta* 43, 869–884.
- Murowchick, J.B., Coveney Jr., R.M., Grauch, R.L., Eldridge, C.S., Shelton, K.L., 1994. Cyclic variations of sulfur isotopes in Cambrian stratabound Ni–Mo–(PGE–Au) ores of southern China. *Geochim. Cosmochim. Acta* 58, 1813–1823.
- Nozaki, Y., 1997. A fresh look at element distribution in the North Pacific Ocean. *Eos Trans. Am. Geophys. Union* 78, 221. <http://dx.doi.org/10.1029/97EO00148>.
- Orberger, B., Vymazalová, A., Wagner, C., Fialin, M., Gallien, J.P., Wirther, R., Pašava, J., Montagnac, G., 2007. Biogenic origin of intergrown Mo–sulphide-and carbonaceous matter in Lower Cambrian black shales (Zunyi Formation, southern China). *Chem. Geol.* 238, 213–231.
- Park, J.W., Hu, Z.C., Gao, S., Campbell, I.H., Gong, H.J., 2012. Platinum group element abundances in the upper continental crust revisited—new constraints from analyses of Chinese loess. *Geochim. Cosmochim. Acta* 93, 63–76.
- Pašava, J., 1993. Anoxic sediments – an important environment for PGE – an overview. *Ore Geol. Rev.* 8, 425–445.
- Pašava, J., Vymazalová, A., Petersen, S., Herzig, P., 2004. PGE distribution in massive sulfides from the PACMANUS hydrothermal field, eastern Manus basin, Papua New Guinea: implications for PGE enrichment in some ancient volcanogenic massive sulfide deposits. *Miner. Depos.* 39, 784–792.
- Pašava, J., Vymazalová, A., Petersen, S., 2007. PGE fractionation in seafloor hydrothermal systems: examples from mafic- and ultramafic-hosted hydrothermal fields at the slow-spreading Mid-Atlantic Ridge. *Miner. Depos.* 42, 423–431.
- Pašava, J., Křibek, B., Vymazalová, A., Šýkorová, I., Žák, K., Orberger, B., 2008. Multiple sources of metals of mineralization in Lower Cambrian black shales of South China: evidence from geochemical and petrographic study. *Resour. Geol.* 58, 25–42.
- Pašava, J., Frimmel, H., Taiyi, L., Koubova, M., Martunek, K., 2010. Extreme PGE concentrations in Lower Cambrian acid tuff layer from the Kunyang phosphate deposit, Yunnan province, south China—possible PGE source for lower Cambrian Mo–Ni–polyelement ores. *Econ. Geol.* 105, 1047–1056.
- Pašava, J., Zaccarini, F., Alglersperger, T., Vymazalová, A., 2013. Platinum-group elements (PGE) and their principal carriers in metal-rich black shales: an overview with a new data from Mo–Ni–PGE black shales (Zunyi area, Guizhou Province, south China). *J. Geosci. Czech.* 58, 209–216.
- Qi, L., Hu, J., Gregoire, D.C., 2000. Determination of trace elements in granites by inductively coupled plasma mass spectrometry. *Talanta* 51, 507–513.
- Qi, L., Gao, J.F., Huang, X.W., Hu, J., Zhou, M.F., Zhong, H., 2011. An improved digestion technique for determination of platinum group elements in geological samples. *J. Anal. At. Spectrom.* 26, 1900–1904.



- Rudnick, R.L., Gao, S., 2003. Composition of the continental crust. *Treatise Geochem.* 3, 1–6. <http://dx.doi.org/10.1016/B0-08-043751-6/03016-4>.
- Sawlowicz, Z., 1993. Iridium and other platinum-group elements as geochemical markers in sedimentary environments. *Palaeogeogr. Palaeoclimatol. Palaeoecol.* 104, 253–270.
- Scott, C., Loyens, T.W., 2012. Contrasting molybdenum cycling and isotopic properties in euxinic versus non-euxinic sediments and sedimentary rocks. Refining the paleoproxies. *Chem. Geol.* 324–325, 19–27.
- Seewald, J.S., Seyfried Jr., W.E., 1990. The effect of temperature on metal mobility in subseafloor hydrothermal systems: constraints from basalt alteration experiments. *Earth Planet. Sci. Lett.* 101, 388–403.
- Shi, C.H., Cao, J., Hu, K., Bian, L.Z., Yao, S.P., Zhou, J., Han, S.C., 2014. New understandings of Ni–Mo mineralization in early Cambrian black shales of South China: constraints from variations in organic matter in metallic and non-metallic intervals. *Ore Geol. Rev.* 59, 73–82.
- Steiner, M., Wallis, E., Erdtmann, B.D., Zhao, Y.L., Yang, R.D., 2001. Submarine-hydrothermal exhalative ore layers in black shales from South China and associated fossils—insights into a Lower Cambrian facies and bio-evolution. *Palaeogeogr. Palaeoclimatol. Palaeoecol.* 169, 165–191.
- Tribouillard, N., Algeo, T.J., Lyons, T., Riboulleau, A., 2006. Trace metals as paleoredox and paleoproductivity proxies: an update. *Chem. Geol.* 232, 12–32.
- Tribouillard, N., Algeo, T.J., Baudin, F., Riboulleau, A., 2012. Analysis of marine environmental conditions based on molybdenum–uranium covariation—applications to Mesozoic paleoceanography. *Chem. Geol.* 324–325, 46–58.
- Wood, S.A., 2002. The aqueous geochemistry of the platinum-group elements with applications to ore deposit. In: Cabri, L.J. (Ed.), *The Geology, Geochemistry, Mineralogy and Mineral Beneficiation of Platinum-Group Elements*. Canadian Institute of Mining, Metallurgy and Petroleum, Spec. vol. 54, pp. 211–249.
- Wood, S.A., Caerar, D.A., Borcsik, M.P., 1987. Solubility of the assemblage pyrite–pyrrhotite–magnetite–sphalerite–galena–gold–stibnite–bismuthinite–argentite–molybdenite in H<sub>2</sub>O–NaCl–CO<sub>2</sub> solutions from 200 to 350 °C. *Econ. Geol.* 82, 1864–1887.
- Wu, B., Xu, L.Q., 2010. Pb–Zn deposits geological characteristics and composition fabric of ore in Guizhou Nayong Shuidong. *J. Guizhou Univ. (Nat. Sci.)* 27, 43–49 (in Chinese with English abstract).
- Wu, C.D., Chen, Q.Y., Lei, J.J., 1999. The genesis factors and organic petrology of black shale series from the upper Sinian to the lower Cambrian, southwest of China. *Acta Petrol. Sin.* 15, 453–462.
- Xu, L.G., Lehmann, B., Mao, J.W., 2012. Seawater contribution to polymetallic Ni–Mo–PGE–Au mineralization in Early Cambrian black shales of South China: Evidence from Mo isotope, PGE, trace element, and REE geochemistry. *Ore Geol. Rev.* 52, 66–84.
- Zhang, G.D., Li, J.L., Xiong, Q.Y., Qi, F., Zeng, M.G., 2002. Enrichment features and patterns of PGE metals in black shale from Zunyi area, Guizhou Province. *Miner. Depos.* 21, 377–386 (in Chinese with English abstract).
- Zhang, G.D., Li, J.L., Xiong, Q.Y., 2005. Platinum-group elements in Cambrian black shale in southern China: differential enrichment of platinum and palladium. In: Mao, J.W., Bierlein, F.P. (Eds.), *Mineral Deposit Research: Meeting the Global Challenge*. Springer, New York, pp. 219–222.
- Zhang, Z., Zhang, B.G., Hu, J., Yao, L.B., Tian, Y.F., 2007. A preliminary discussion on the biometallogenesis of TI deposits in the low-temperature minerogenetic province of southwestern China. *Sci. China Earth Sci.* 50, 359–370.